International Journal of Advanced Engineering, Management and Science (IJAEMS)
Peer-Reviewed Journal
ISSN: 2454-1311 | Vol-9, Issue-4; Apr, 2023
Journal Home Page: https://ijaems.com/
Article DOI: https://dx.doi.org/10.22161/ijaems.94.2

Behavior of Composite Piles Reinforced by Geosynthetics

El-Sayed A. El-Kasaby[1a], Mohab Roshdy [1b], Mahmoud Awwad [1c], Mona I. Badawi [1*]

Civil Engineering Department Benha Faculty of Engineering, Benha University, Cairo, Egypt
[a] Prof. of soil mechanics and foundations. Email. Profkassaby@gmail.com
[b] Lecturer. Email. Mohab.elashmouny@bhit.bu.edu.eg
[c] Lecturer. Email. mahmoud.awad@bhit.bu.edu.eg
[*] Teaching Assistant. PhD Student. Email. Mona.ibrahim@bhit.bu.edu.eg

Received: 15 Mar 2023; Received in revised form: 10 Apr 2023; Accepted: 18 Apr 2023; Available online: 26 Apr 2023

***Abstract*— *This study presents the results of five reinforced concrete (RC) pile specimens that were created and horizontally loaded. The RC piles were reinforced by composite materials such as geogrid, geogrid with a core of steel rod, and geogrid with a core of glass fibre reinforced polymers (GFRP) or carbon fiber reinforced polymers (CFRP) rod. This research is expected to investigate the behavior of using composite materials in pile reinforcement and check their efficiency in carrying horizontal loads. The horizontal pile loading test was applied to four pile specimens and a reference pile specimen reinforced by steel rods. All specimens have the same dimensions (150 mm in diameter and 1050 mm in height). A comparison has been carried out between the experimental results for all specimens and the reference specimen. The experimental results illustrated that the specimens carried a lower ultimate horizontal load by 44%–87% compared to the reference specimen. Also, a non-linear finite element analysis has been verified by Abaqus software and achieved a great degree of reconciliation compared to the experimental results. Finally, a comparison of the reinforcement costs for the specimens revealed that utilizing these composite piles could reduce the cost up to 15.2%.*

***Keywords*— Geosynthetics Geogrid, Composite piles, Horizontal load**

I. INTRODUCTION

In recent years, a relatively new trend in deep foundations is the use of composite piles due to their inherent advantages over traditional piles. Composite piles refer to alternative pile foundations composed of fiber reinforced polymers (FRPs) or geosynthetic that are placed into the ground to support axial and horizontal loads [1]. Geosynthetics geogrids was proved to be a promising material in replacing traditional pile materials such as concrete and steel. Development and use in other industries have driven the price of production down to an attractive price point and produced a commercially viable technology [2]. Composite piles with fiber-reinforced polymers (FRP) are a suitable solution to the problems faced by traditional piles as illustrated in several studies [3-13]. Omar Alajarmeh et al. (2020) investigated the use of glass fiber reinforced polymer (GFRP) rods as a solution for corrosion and the use of hollow composite reinforced sections (HCRSs) to confine the inner concrete wall in HCCs [14]. AlAjarmeh O.S. et al. (2019) explored the use of GFRP composite rods as reinforcement for HCCs and evaluated the effect of the reinforcement ratio on HCC structural behavior. Their results showed that increasing the diameter and number of rods enhanced the strength, ductility and confinement efficiency of HCC. For columns with equal reinforcement ratios, using more and smaller-diameter GFRP rods yielded 12% higher confinement efficiency than in the columns with fewer and larger-diameter rods. The crushing strain of the GFRP rods embedded in the HCC was 52.1% of the ultimate tensile strain [15]. Previous studies related to the performance of hollow FRP piles only include superficial consideration of the impact behavior of the fiber materials and do not systematically describe their impact strength. These studies described the impact behavior of the fiber composite materials through the observed damage mechanisms only [16][17]. Ahmed H. Ali et al. (2020) presented a numerical analysis investigation, using finite element model (FEM) and modified compression field theory (MCFT), which was conducted to evaluate the shear capacity and behavior of circular concrete piles reinforced with steel and FRP rods by considering shear behavior, shear strength, and deflection shape [18]. Pando et al. (2006) carried out a large-scale pile load test investigating the performance of FRP piles as the supporting structure for a highway overpass in Virginia. They compared driven precast concrete piles to concrete in-filled FRP piles. Axial pile load tests showed that the FRP piles performed comparably to the concrete pile [19].

This study targeted to examine a new technique for reinforcing piles by using different materials and check their efficiency under horizontal loads(H). horizontal pile loading tests was applied on five piles as reference concrete pile (PSH) reinforced by steel rods, a concrete pile (PGH) reinforced by geosynthetics geogrids (G), and concrete piles (PSGH, PLGH, PCGH) reinforced by geosynthetics geogrids with a core of steel rod in the middle. Also, the costs of the specimens were compared.

Nomenclature	
P	***pile***
S	***steel rod***
L	***glass fiber rod***
C	***carbon fiber rod***
G	***geogrid***
H	***horizontally loaded***

II. EXPERIMENTAL PROGRAM

2.1 Specimens and Test Matrix

five specimens were contained in the experimental program as shown in table 1. The pile specimens were constructed and tested. The tested specimens included five reinforced concrete piles with the same dimensions (150 mm in diameter x 1050 mm in height). The reference pile specimen was reinforced using high tensile steel that formed of four rods with 8 mm diameter and a spiral stirrup of mild steel with 6 mm diameter. The second pile specimen PGH was reinforced using G formed as a cylindrical roll. The other three pile specimens (PSGH, PLGH, and PCGH) were reinforced by cylindrical roll of geogrid with a core of steel, GFRP or CFRP rod in the middle. The horizontally loading test was applied on all specimens. The reinforcing schemes used in the present study according to the previous explanation was shown in figure 1. The variables of the experimental program were the materials used in the reinforcement and the combination of two materials.

Table 1. Test matrix

Group No.	Pile Code	Conditions	Loading Type	Applied Material
Reference	**PSH**	**Reference**		**Steel Rods (S)**
	PGH		**Horizontal load**	**Geogrid (G)**
	PSGH			**Steel Rod (S) & Geogrid (G)**
	PLGH			**Glass Fiber Rod (L) & Geogrid (G)**
	PCGH			**Carbon Fiber Rod (C) & geogrid (G)**

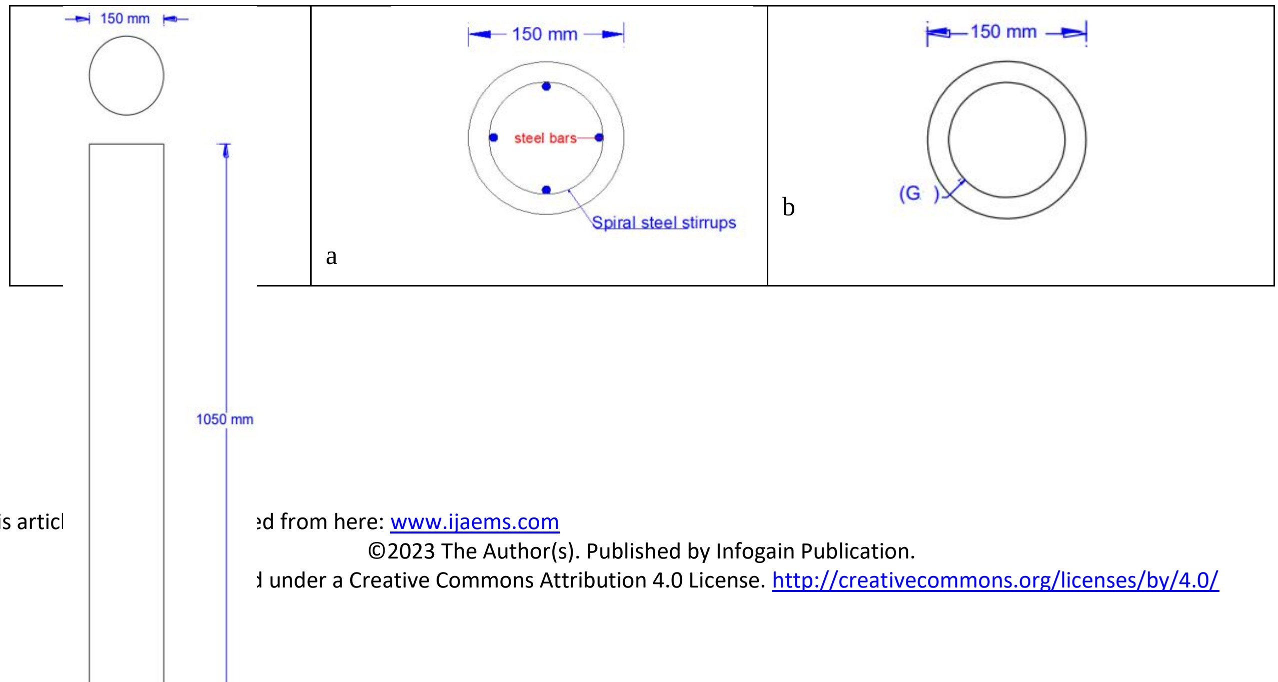

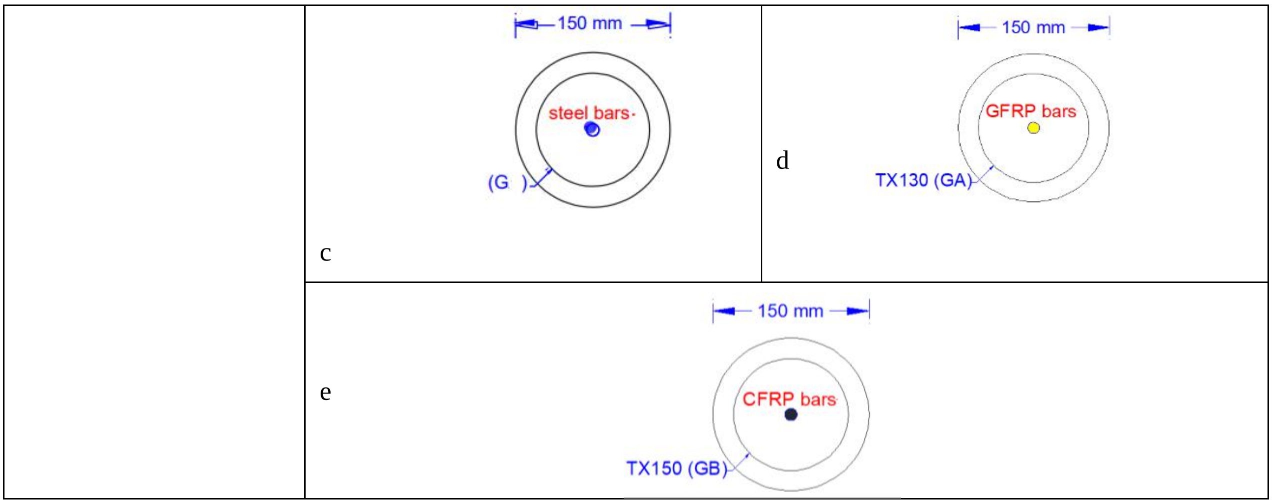

Fig.1 Cross section of composite pile specimens.

(a) Reference pile PSH, (b) PGH, (c) PSG, (d) PLGH, (e)PCGH.

2.2 Material Properties

Ordinary Portland Cement (OPC-42.5 grade), and natural sand with 2.6 fineness moduli with filter stones having a maximum aggregate size of 9 mm were used in the tested specimens. At 28 days, the predicted compressive strength (fcu) was 25 MPa. The actual fcu was gained on the day of testing.

High tensile steel rods grade (40) having 8 mm diameters was used as the main reinforcement of the tested piles. Normal mild steel rods grade (36) was used for spiral stirrups having 6 mm diameter. The reference concrete pile was reinforced with 6 mm diameter normal mild steel as spiral stirrups and 8 mm diameter high tensile steel rods as vertical reinforcement.

GFRP rods used in this research were manufactured by Russian company Armastek and imported by Fiber Reinforcement Industries Company [22]. According to the manufacturer, the mechanical properties of the GFRP rods were given in Table 2.

Geosynthetics Geogrid manufactured by Tensar International Corporation and imported by National Geotechnical Company for (GEOTECH) [23]. Table 2 gives the mechanical properties of geogrid, according to the manufacturer.

Table 2. Dimensions and characteristic properties of FRP rods. [22],[23]

Features	***Geogrid (G)***	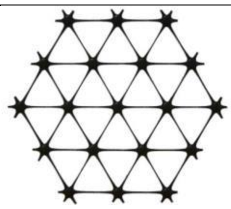
Thickness (mm)	1.3	
Tensile strength (N/mm)	10	
Modulus of elasticity (MPa)	200000	
Strain at failure	0.5%	
Features	***GFRP rod (L)***	
Diameter (mm)	12	
Tensile strength (MPa)	1100	
Modulus of elasticity (MPa)	45000	
Strain at failure	2.2%	
Features	***CFRP rod (C)***	
Diameter (mm)	12	
Tensile strength (MPa)	1050	
Modulus of elasticity (MPa)	120000	
Strain at failure	0.5%	

2.3 Test Set-Up

The specimens were loaded with a hydraulic jack with a maximum capacity of 1000 (KN), conjoined to electric pump, and suspended with a rigid reaction frame with a maximum capacity of 1000 (KN). The horizontal loaded specimens were placed on two I beam at both sides; one beam represented the pile cap and the other represented the end bearing layer. The load was transferred horizontally by a steel rod to the pile surface using steel plate. The applied loads were measured by a load cell with a maximum capacity of 1000 (KN) located below the hydraulic jack. To monitor displacement for the horizontal loaded specimens, one Linear Variable Differential Transducer (LVDT) was installed beneath the upper third of the pile surface. All test data were collected with a data acquisition system and collected on a computer at two-second intervals. Figure 2 showed the tests setup which was applied in the concrete laboratory of Benha Faculty of Engineering at the University of Benha.

III. EXPERIMENTAL RESULTS AND DISCUSSION

3.1 Ultimate Horizontal Load.

Table 3 presented the ultimate horizontal load (N), deflection at failure (mm), and the cost of reinforcement (L.E.) for tested pile specimens PSH, PGH, PSGH, PLGH, PCGH. The relationship between the horizontal load against the deflection for the experimented pile specimens PSH, PGH, PSGH, PLGH and PCGH was shown in fig. 4.

Table 3. Experimental results

Group No.	Pile Code	Ultimate Horizontal Load (KN)	Ultimate Load/ Ultimate load of PSH %	Deflection at Failure (mm)	Price of Reinforcement (L.E.)	Price of Reinforcement compared to PSH %
Reference	PSH	27.853	Reference Pile	11.30	40	-
	PGH	12.205	44	5.45	6.15	15.25
	PSGH	21.302	76.5	7.35	23.95	59.65
	PLGH	23.655	85	8.7	14.15	35.25
	PCGH	24.21	87	18.5	106.15	265.3

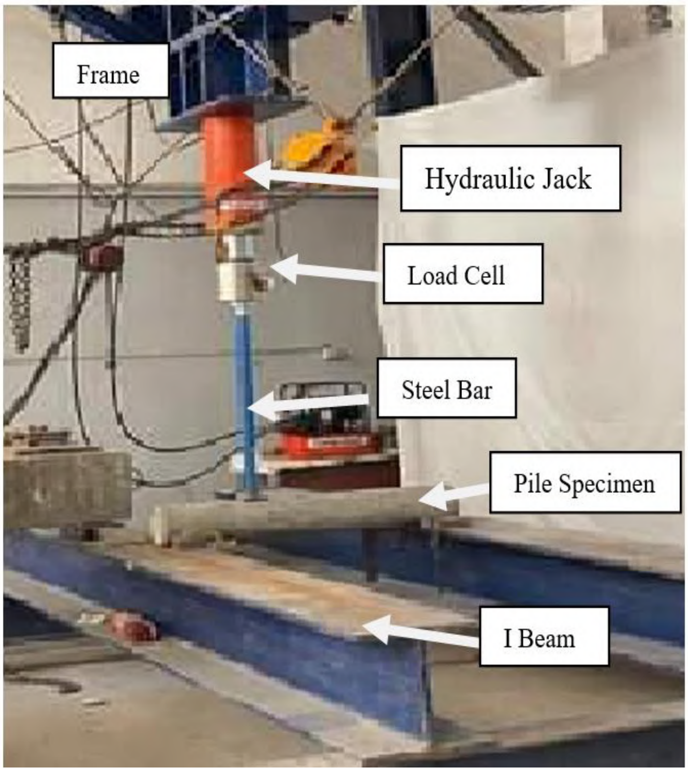

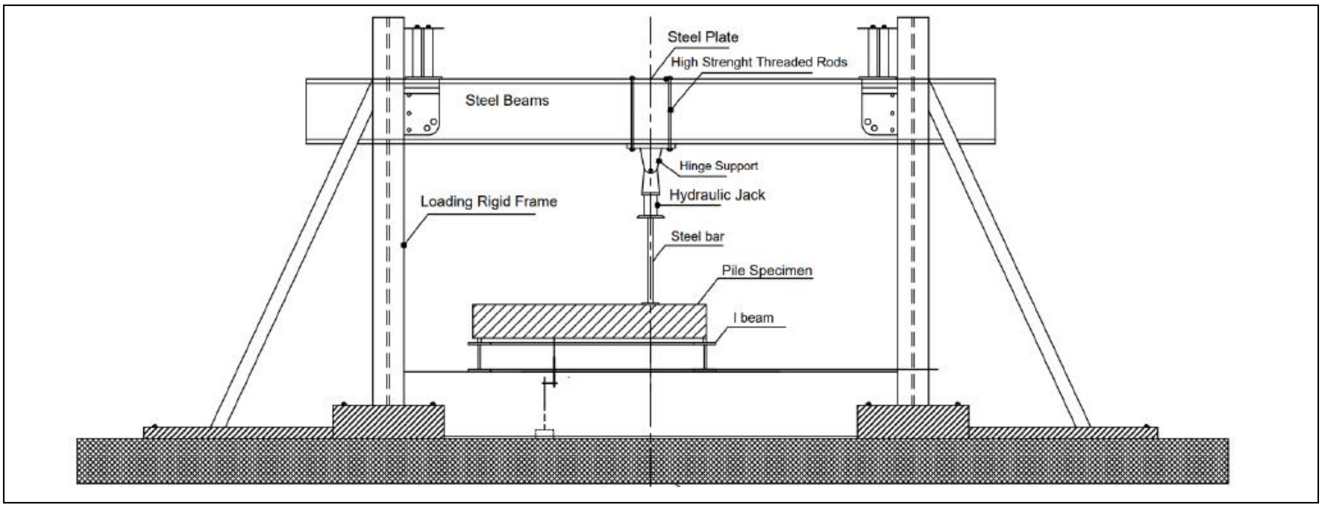

Fig.2 Horizontally loaded test set-up.

3.2 *Results and Discussion for Ultimate Horizontal Load*

The ultimate horizontal loads for pile specimens PGH, PSGH, PLGH, and PCGH achieved a change of 44%, 76.5%, 85%, and 87% respectively compared to reference pile specimen PSH as shown in Table 3, the use of geogrid resulted a decrease in the ultimate horizontal load, the ultimate horizontal load was decreased to 44% of the reference specimen using geogrids. Also, it was decreased to 76.5% of the reference pile specimen using a core of steel rod with geogrid, while it was decreased to 85% using a core of GFRP rod with geogrid and decreased to 87% using a core of CFRP rod with geogrid. It can be noted that the core of the steel rod or GFRP rod increased the horizontal load with the geogrid.

Comparing the specimens reinforced with different materials and loaded by horizontal load as shown in figure 6, it can be noted that the ultimate horizontal load was decreased using geogrid with or without a core of (steel, GFRP, CFRP) rod. The reason for this decrement was its ability to make confinement with low tensile strength. It can be noted that using a core of steel rod increased the ultimate horizonal load by 32.5% compared to using geogrid alone, while using a core of GFRP rod increased the ultimate horizonal load by 41% compared to using geogrid alone and using a core of CFRP rod increased the ultimate horizonal load by 43% compared to using geogrid alone So, using a core of steel rod, GFRP rod or CFRP rod enhanced the horizontal capacity of the pile.

The price of reinforcement for pile specimens PGH, PSGH, PLGH, and PCGH achieved a change of 15.25%, 59.65%, 35.25%, and 265.3% respectively compared to reference pile specimen PSH as shown in Table 3. The price of the reinforcement decreased effectively using the geogrid material alone or with a core of steel or GFRP rod.

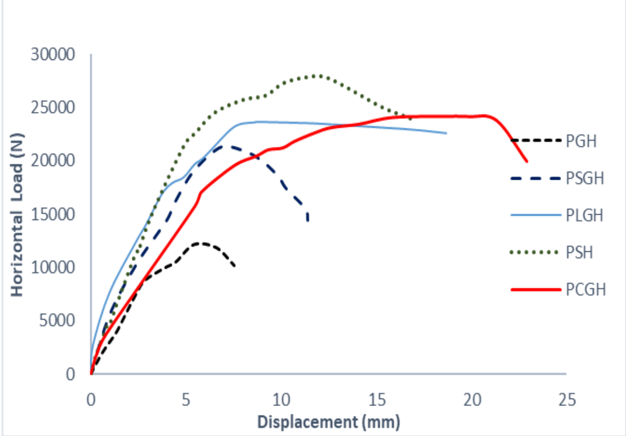

Fig.4 Horizontal load - displacement curve for tested pile specimens PSH, PGH, PSGH, PLGH and PCGH.

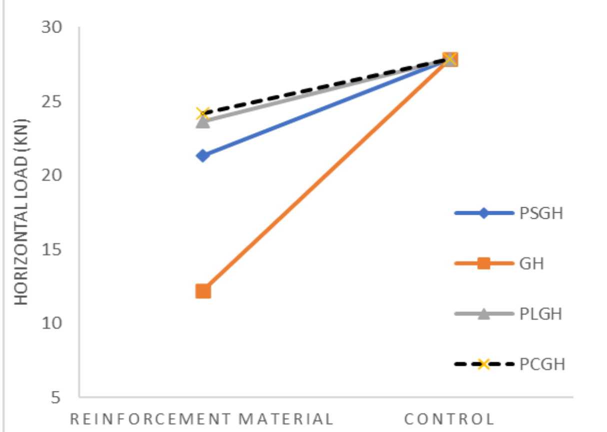

Fig.5 Horizontal load vs reinforcement material relationship for Horizontal loaded specimens

3.3 *Modes of Failure*

For the reference specimen, the mode of failure acted a ductile failure by tension. For geogrid, or geogrid with a core of steel rod or GFRP rod the modes of failure were a ductile failure by tension, while for geogrid with a core of steel rod, the mode of failure acted a brittle failure by tension. The modes of failure for all specimens are shown in fig. 6.

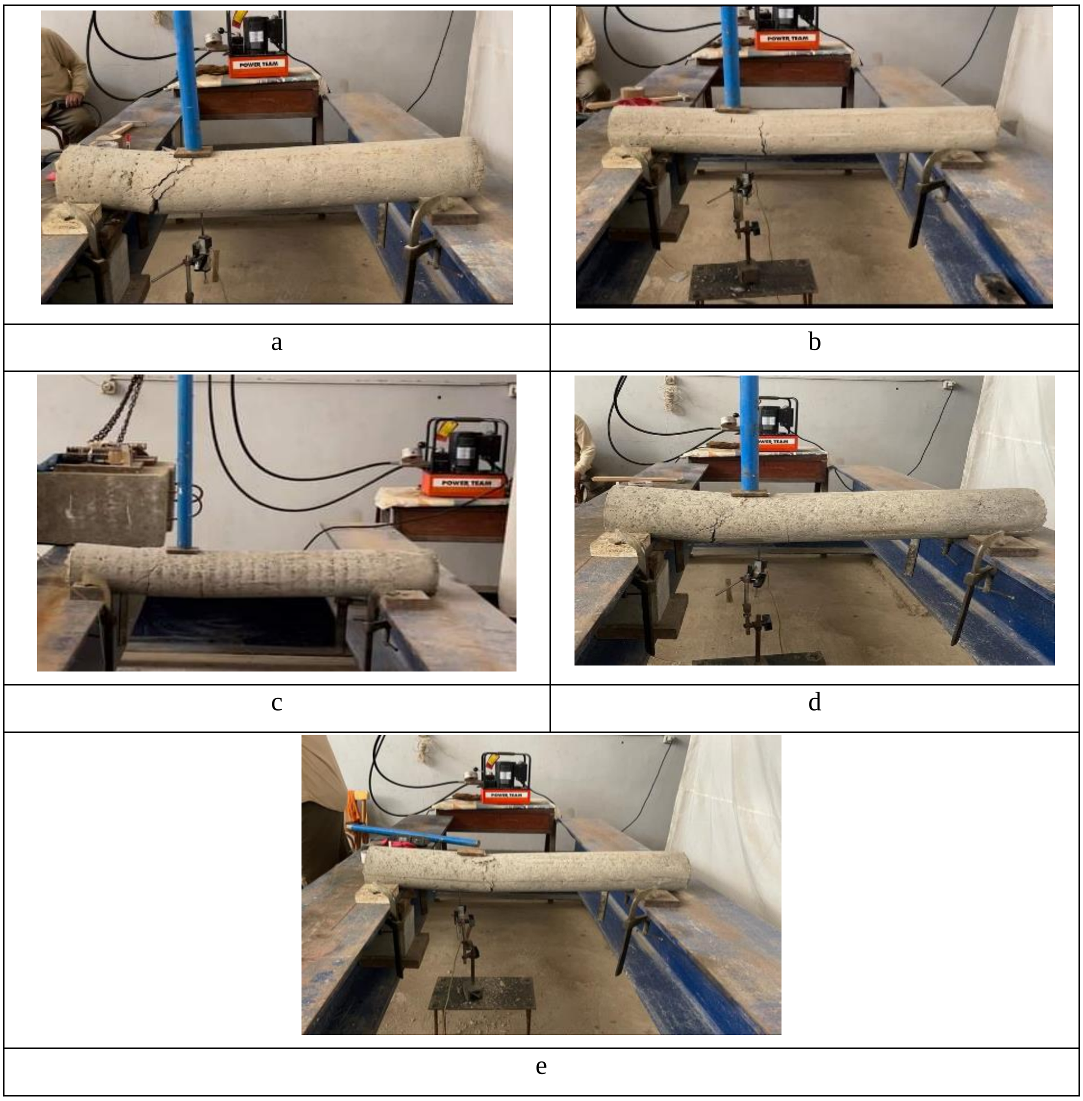

Fig.6 Modes of failure for horizontal loaded specimens

a) PSH b) PGH, c) PSGH, d) PLGH and e) PCGH.

IV. FINITE ELEMENT ANALYSIS

Using a finite-element software Abaqus/CAE standard 6.14-2, a finite-element (F.E) analysis was performed to simulate the behavior of concrete piles reinforced with different materials (steel rods, geogrid and geogrid with steel, CFRP or GFRP rod) under the effect of horizontal load. A lot of features were considered in the F.E.M. as, each part of the model, material properties, the assembly for modeling, the steps of modeling, the contact between the model parts, condition of loading, meshing of the model, and finally solving the model.

The same material properties applied in the experimental program for the concrete, steel, CFRP, GFRP rods, and geogrids were inputted into the Abaqus software to reproduce the experimental program. The material properties factors were considered in modeling, such as concrete compressive strength, steel, CFRP and GFRP, geogrid tensile strength. A solid part was used to model the concrete. A wire parts were used to model the reinforcement as steel, CFRP or GFRP rods and a shell planar part was used to model the geogrid shell. In the concrete pile, the reinforcement elements were inserted as embedded elements. In the F.E.M, the load was applied horizontally. The modeling of the horizontal loaded pile specimens was shown in figure 7.

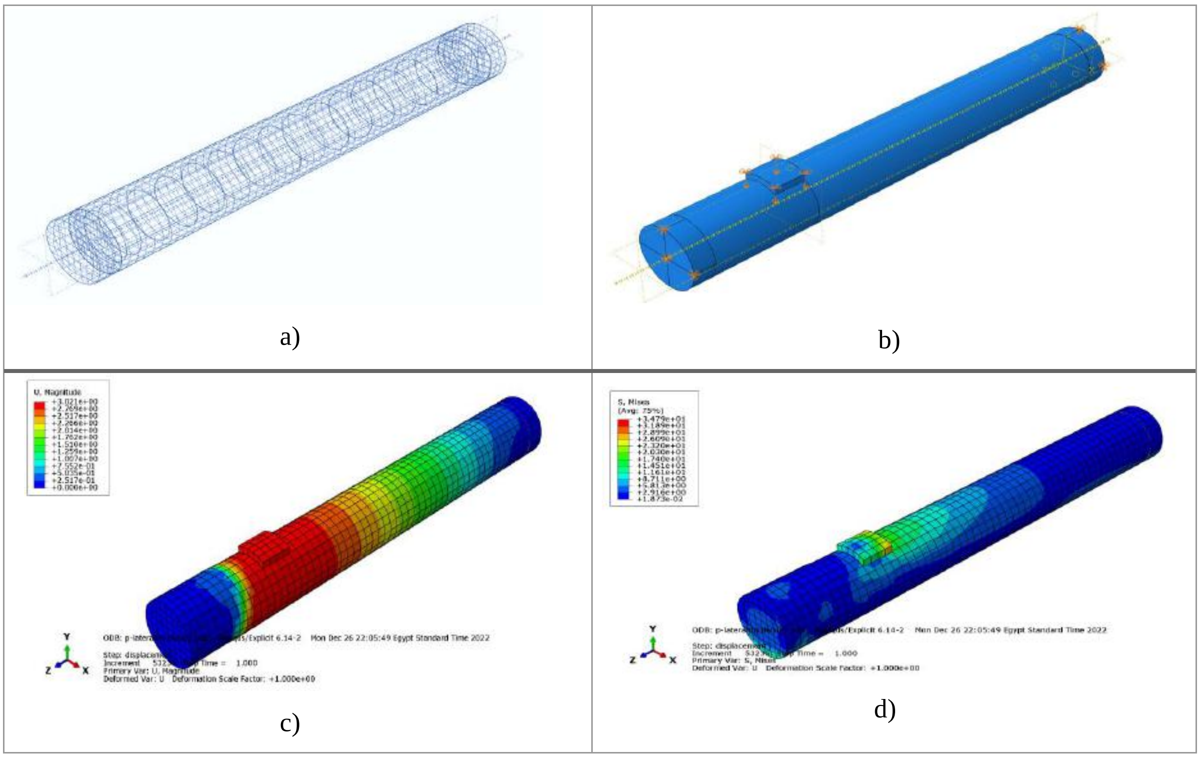

Fig.7 Simulating of horizontal loaded pile specimens.

a) Meshing of the model, b) Loading case, c) The deflection on the model, d) Stresses on the model.

The results gained from the FE modeling were verified with the experimental results. The FE model was used for the verification process of the pile specimens (PSH, PGH, PSGH, PLGH, PCGH). The horizontally loaded specimens PSH, PGH, PSGH, PLGH and PCGH achieved a change in ultimate horizontal load of 107.89%, 99.1%, 101.39% 102.94%, and 101.1% respectively compared to the reference specimen PSH. The experimental, and the FEM ultimate horizontal load results were shown in table (4) and achieved a great convergence as shown. Figure 8 presented the load-deflection curves for the experimental and FEM results of the specimens respectively.

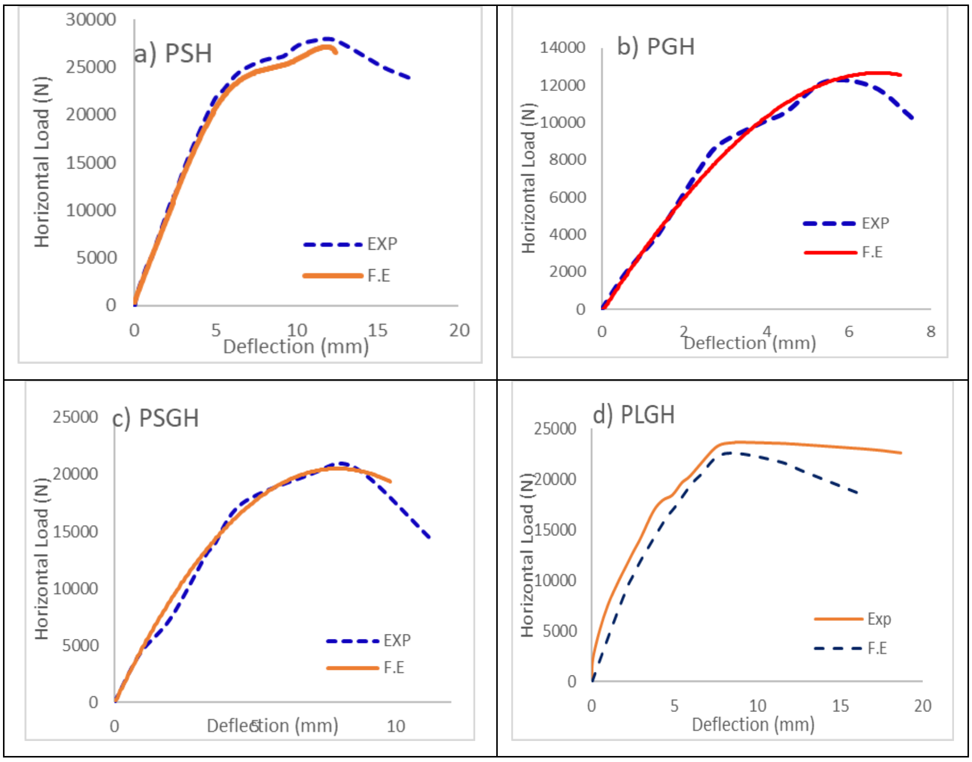

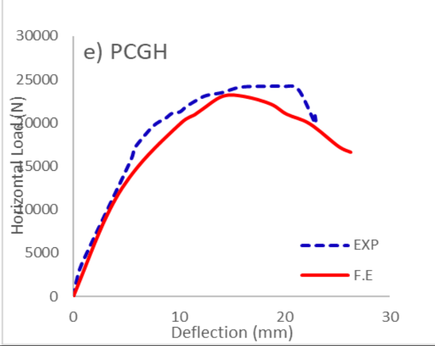

Fig.8 Horizontal load –Displacement relationship for experimental and FEM.

Table 4. Experimental, and FEM results.

Pile Code	V_{EXP} (KN)	V_{FE}. (KN)	V_{EXP}. /V_{FE}
PSH	27.85	25.82	1.08
PGH	12.21	12.31	0.99
PSGH	21.30	21.01	1.01
PLGH	23.66	22.98	1.03
PCGH	24.21	23.95	1.01
	Mean		1.02
	SD		0.0331
	Covariance		0.0011

V. ANALYTICAL CALCULATIONS

All specimens were horizontally loaded. the ultimate predicted horizontal load of the control specimen (pile reinforced with steel rods) can be estimated by applying in equation (1) according to ECP 201 (201) [20] and using interaction diagrams for design circular section under moment.

$M_u = (K\times e/R) \times R^3 \times f_{cu}$ (KN.m) (1)

Up to now, the ultimate horizontal load of piles reinforcement by geogrids cannot be estimated by ECP 201 (201) [30]. The following paragraph presents suggested equation for specimens reinforced with geogrids which estimated the ultimate horizontal moment by applying in Equation (2). Where, α_s is a reduction factor depends on the position of the reinforcement rod and α_G is a reduction factor depends on the geogrid material. Table (6) presents a comparison between experimental and theoretical results which listed in the same table. A great convergence was verified from the theoretical and experimental results.

$M_u = (\alpha_G\times(K\times e/R) \times R^3 \times f_{cu}) + (\alpha_s\times(K\times e/R) \times R^3 \times f_{cu})$(KN.m) (2)

Where:

M_u Ultimate horizontal moment on the specimen

V_u Ultimate horizontal load on the specimen

f_{cu}: concrete compressive strength.

$K\times e/R$: factor depends on the ratio of reinforcement and the radius of the specimen that can be estimated from the interaction diagram according to ECP 201 (201) [20].

R: the radius of the specimen.

α_s: reduction factor depends on the position of the reinforcement rod.

α_s =1 for steel rods on the edges, α_s = 0.45 in the center, α_s = 0.75 for FRP rods.

α_G reduction factor depends on the material.

α_G = 0.45 for the geogrid used.

Table 6: Comparison of Experimental and Theoretical Results.

Pile Code	V_{EXP} (KN)	$V_{th.}$ (KN)	$V_{EXP.}/V_{th}$
PSH	27.853	26.52	1.005
PGH	12.205	11.934	1.095
PSGH	21.302	21.024	0.984
PLGH	23.655	23.25	1.018
PCGH	24.21	23.8	1.01
	Mean=		1.022
	SD=		0.04299
	Covariance =		0.001848

VI. CONCLUSION

- Using geogrid as reinforcement didn't enhance the ultimate horizontal load of the pile.
- The ultimate horizontal load was decreased by 44%- 87% for specimens reinforced by geogrids with or without a core of (steel GFRP or CFRP) rod, but the core of steel, GRFP or CFRP rod was effective in withstanding horizontal load with the geogrid.
- The cost of the reinforcement decreased effectively for the pile specimens reinforced by geogrids and geogrid with a core of steel or GFRP rod, but it increased effectively using a core of CFRP.
- Non-linear finite Element analysis has been verified and achieved a great convergence against the experimental results.
- A theoretical equation has been suggested to predict the ultimate horizontal load which achieved a great convergence with the experimental results.

REFERENCES

[1] Guades E., Aravinthan T., Islam M., and Manalo A., (2012), "A review on the driving performance of FRP composite piles", Compos Struct, ELSEVIER, Volume 94, Pages 932–1942.

[2] Giraldo J., and Rayhani M. T., (2014), "Load transfer of hollow Fiber-Reinforced Polymer (FRP) piles in soft clay", Elsevier, Transportation Geotechnics, Volume 1, Pages 63–73.

[3] Afifi M. Z., Mohamed H. M., and Benmokrane B., (2013), "Axial capacity of circular concrete columns reinforced with GFRP bars and spirals" Journal of Composites for Construction Volume 25.

[4] Paramanantham N. S., (1993), "Investigation of the behavior of concrete columns reinforced with fiber reinforced plastic rebars", Lamar University.

[5] Alsayed S. H., Al-Salloum Y. A., Almusallam T. H., and Amjad M. A., (1999), "Concrete columns reinforced by glass fiber reinforced polymer rods", Special Publication. Volume 188, Pages 3-12.

[6] De Luca A., Matta F., and Nanni A., (2010), "Behavior of full-scale glass fiber-reinforced polymer reinforced concrete columns under axial load", ACI Structural Journal. Volume 107.

[7] Pantelides C. P., Gibbons M. E., Reaveley L. D., (2013), "Axial load behavior of concrete columns confined with GFRP spirals", Journal of Composites for Construction, Volume 17.

[8] Suresha, K. (2022). Electron Diffusion and Phonon Drag Thermopower in Silicon Nanowires. In International Journal of Chemistry, Mathematics and Physics (Vol. 6, Issue 1, pp. 01–04). AI Publications. https://doi.org/10.22161/ijcmp.6.1.1

[9] Mohamed H. M., Afifi M. Z., Benmokrane B., (2014) "Performance evaluation of concrete columns reinforced longitudinally with FRP bars and confined with FRP hoops and spirals under axial load", Journal of Bridge Engineering. Volume 19.

[10] Tobbi H., Farghaly A. S., and Benmokrane B., (2014), "Behavior of concentrically loaded fiber-reinforced polymer reinforced concrete columns with varying reinforcement types and ratios", ACI Structural Journal Volume 111.

[11] Hales T. A., Pantelides C. P., and Reaveley L. D., (2016), "Experimental Evaluation of Slender High-Strength Concrete Columns with GFRP and Composite Reinforcement", Journal of Composites for Construction.

[12] Hadi M. N., and Youssef J., (2016), "Experimental Investigation of GFRP-Reinforced and GFRP-Encased Square Concrete Specimens under Axial and Eccentric Load, and Four-Point Bending Test", Journal of Composites for Construction, Volume 20.

[13] Karim H., Sheikh M. N., Hadi M. N., (2016), "Axial load-axial deformation behaviour of circular concrete columns reinforced with GFRP bars and helices", Construction and Building Materials, Volume 112.

[14] Hadi M. N., Karim H., and Sheikh M. N., (2016), "Experimental investigations on circular concrete columns reinforced with GFRP bars and helices under different loading conditions", Journal of Composites for Construction, Volume 9.

[15] Alajarmeh O., Manalo A., Benmokrane B., Ferdous W., Mohammed A, Abousnina R., Elchalakani M., Edoo A., (2020) "Behavior of circular concrete columns reinforced with hollow composite sections and GFRP bars", Marine Structures, ElSEVIER, Volume 72.

[16] AlAjarmeh O. S., Manalo A. C., Benmokrane B., Karunasena W., and Mendis P., (2019), "Axial

Performance of Hollow Concrete Columns Reinforced with GFRP Composite Bars with Different Reinforcement Ratios," Composite Structures, ElSEVIER, Volume 213, Pages 153-164.

[17] Guades E. J., Aravinthan T., and Islam M. M., (2011), "Driveability of composite piles", In: Proceedings of the 1st intl postgraduate conference on eddBE2011, Brisbane, Australia, p. 237–42.

[18] Mirmiran A., and Shahawy Y. S. (2002), "Analysis and field tests on the performance of composite tubes under pile driving impact", Compos Struct, Volume 55.

[19] Ali A. H., Goudaa A., Mohameda H. M., Rabiea M. H., Benmokraneb B. (2020), "Nonlinear finite elements modeling and experiments of FRP-reinforced concrete piles under shear loads", Structures, ElSEVIER, Volume 28, Pages 106-119.

[20] Moussa, M. B., Abdellaoui, M., & Lamloumi, J. (2021). Determination of the hydrogen coefficient diffusion DH in the MmNi3.55Mn0.4Al0.3Co0.75-xFex ($0 \leq x \leq 0.75$) electrodes alloys by cyclic voltammetry. In International Journal of Chemistry, Mathematics and Physics (Vol. 5, Issue 5, pp. 1–6). AI Publications. https://doi.org/10.22161/ijcmp.5.5.1

[21] Pando A. M., Ealy C. D., Flitz M. G., Lesko J. J., and Hoppe E. J., (2006), "A laboratory and field study of composite piles for bridge substructures", McLean, VA: Federal Highway Administration, Report No. FHWA-HRT04-043.

[22] ECP-Egyptian Code of Practice-201. (2011), "Egyptian code of Practice", No. 201 for calculating loads and forces in structural work and masonry, National Research Center for Housing and Building, Ministry of Housing, Utilities and Urban Planning, Cairo.